JACS
JOURNAL OF THE AMERICAN CHEMICAL SOCIETY
Article
pubs.acs.org/JACS

Interpretation of Stochastic Events in Single-Molecule Measurements of Conductance and Transition Voltage Spectroscopy

Ioan Bâldea*

Theoretische Chemie, Universität Heidelberg, D-69120 Heidelberg, Germany, and National Institute for Laser, Plasma and Radiation Physics (NILPRP), Institute for Space Science (ISS), Bucharest-Măgurele RO-077125, Romania

Supporting Information

ABSTRACT: The first simultaneous measurements of transition voltage (V_t) spectroscopy (TVS) and conductance (G) histograms (Guo et al., *J. Am. Chem. Soc.* **2011**, *133*, 19189) form a great case for studying stochastic effects, which are ubiquitous in molecular junctions. Here an interpretation of those data is proposed that emphasizes the different physical content of V_t and G and reveals that fluctuations in the molecular orbital alignment have a significantly larger impact on G than initially claimed. The present study demonstrates the usefulness of corroborating statistical information on different transport properties and gives support to TVS as a valuable investigative tool.

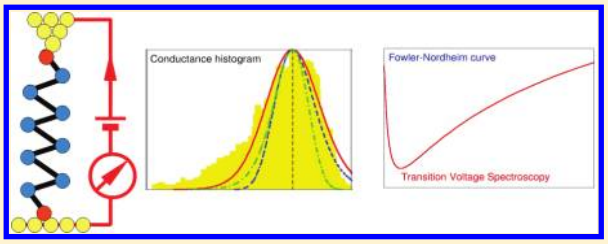

INTRODUCTION

Whatever the fabrication method,[1] the formation of a single-molecule junction is a statistical event subject to stochastic fluctuations. Statistical data analysis is a basic step for extracting confident results and is unavoidable in understanding molecular transport theoretically and in designing molecular devices with desired functions. A prerequisite for this is the ability to conduct a large number (∼thousands) of transport experiments in a short time. Recent experimental achievements in chemically preparing and manipulating break junctions represent a significant advance in this direction.[2−4] Until recently, the statistical analysis of molecular transport data comprised measurements at fixed low biases. The resulting conductance (G) histograms revealed well-known broad peaks[5−9] characterized by a full width at half-maximum (fwhm), ΔG, that is typically larger than the most probable value ($\Delta G > G_{m.p.}$).[3,4,6] The quantitative understanding of the rather broad maxima was confronted with numerous difficulties from both the experimental and theoretical sides, such as impossibility of microscopically characterizing the molecule−electrode contacts (say, hybridization parameters $\Gamma_{s,t}$) and the relative alignment $\varepsilon_0 = E_{MO} - E_F$ between the (frontier) molecular orbitals (MOs) and the electrode Fermi levels.

The parameter ε_0 plays a key role because it controls the charge transport efficiency. To determine ε_0, transition voltage (V_t) spectroscopy (TVS) was recently proposed.[10] Because of its simplicity, it has become a very popular tool in experimental molecular electronics.[2−4,10−15] Theoretical aspects of TVS have also been discussed.[16−21]

Experimental data reveal significant differences between the G and V_t histograms. Transition voltage histograms reported in recent works[2−4] are significantly narrower. They are characterized by standard deviations amounting to $\delta v_t = \delta V_t/V_t^{m.p.} \sim$ 10−20% of the most probable values $V_t^{m.p.}$.[2−4,10,11]

A meaningful analysis of the role played by fluctuations should obviously rely upon G and V_t histograms obtained by simultaneous measurements on the same molecular devices. Such data have been reported in an important recent work.[4] The question of the physical origin of the fluctuations responsible for the different widths of the G and V_t histograms has already been addressed in ref 4. From results of Wentzel−Kramers−Brillouin (WKB) calculations based on the Simmons model[22] and the "barrier shape" conjecture (i.e., that $eV_t \approx |\varepsilon_0|$[10,12,20]), it has been argued that essentially the fluctuations in G are determined by the contacts' resistance and that variations in the energy offset ε_0 play a very reduced role. However, it has been shown that with Simmons-type calculations it is impossible to reproduce quantitatively the $I-V$ curves of molecular junctions based on octanedithiol (ODT) in the higher-voltage range of interest ($V \sim V_t$),[18] and ODT is one of the molecular species employed in ref 4. From a more general perspective, it is worth noting an important shortcoming of the Simmons model: it does not account for the lateral constriction of electron motion and therefore is inappropriate for describing nanoelectronic devices with sharp electrodes.[23]

This indicates that fluctuations in G and V_t are not properly understood at present. Unraveling their physical origin is of general interest for molecular electronics, and this is the main *specific* aim of the present paper. The main *general* aim of this study is to emphasize the usefulness of corroborating statistical information on different transport properties.

COMPUTATIONAL SECTION

For illustration, I will restrict myself here to the high-conductance (H-type) ODT-based junctions of ref 4. The model employed below is the

Received: March 7, 2012

   dx.doi.org/10.1021/ja302248h | J. Am. Chem. Soc. XXXX, XXX, XXX−XXX

Newns–Anderson model, which was extensively employed in chemisorption and electrochemistry[24−26] as well as in recent theoretical studies of TVS.[20,21] The molecular junction is modeled as a single energy level interacting with two electrodes [say, substrate (s) and tip (t)]. Since ODT junctions exhibit p-type conduction,[12] it is the HOMO ($\varepsilon_0 \equiv -\varepsilon_h = E_{HOMO} - E_F < 0$) that is responsible for electric transport. Within the wide-band limit, the width functions $\Gamma_{s,t}$ are energy-independent, and the current I and the conductance per molecule G can be expressed in simple analytical forms:[18,20,26−28]

$$I = \frac{G_0}{e}\frac{\Gamma^2}{\Gamma_a}\left(\arctan\frac{\Lambda_+}{\Gamma_a} - \arctan\frac{\Lambda_-}{\Gamma_a}\right) \tag{1}$$

$$\Gamma_{s,t} = \tau_{s,t}{}^2\mathcal{N}_{s,t}$$
$$\Gamma^2 \equiv \Gamma_s\Gamma_t \tag{2}$$
$$\Gamma_a \equiv (\Gamma_s + \Gamma_t)/2$$

$$g \equiv \frac{G}{G_0} \equiv G_0{}^{-1}\frac{\partial I}{\partial V}\bigg|_{V\to 0} \approx \frac{\Gamma^2}{\varepsilon_h{}^2} \tag{3}$$

In the above, $G_0 = 2e^2/h$, $\tau_{s,t}$ are the molecule–electrode resonance integrals, $\mathcal{N}_{s,t}$ are the electrodes' density of states at the Fermi level, and $\Lambda_\pm \equiv \varepsilon_h \pm eV/2$.

Equation 1 assumes a potential V that symmetrically drops at the contacts and is flat across the molecule (as suggested by ab initio calculations for ODT[29] at biases $V < 2$ V).[18,30] The approximate forms of eq 3 above and eq 4 below hold to order $O(\Gamma_a/\varepsilon_h)^2$ and are very accurate in realistic cases (see below). By using eq 1 and imposing the condition $\partial[\log I(V)/V^2]/\partial(1/V) = 0$ (which defines the Fowler–Nordheim minimum[10]), one obtains two transition voltages $V_{t\pm}$ for positive and negative bias polarities of equal magnitude: $V_{t\pm} = \pm V_t$.[18,20] Straightforward calculations[21] yield the following analytical expressions valid to order $O(\Gamma_a/\varepsilon_h)^4$:

$$eV_t = \frac{2}{\sqrt{3}}\varepsilon_h + \frac{11}{\sqrt{3}}\frac{\Gamma_a{}^2}{3\varepsilon_h} \approx 1.154\varepsilon_h \tag{4}$$

For ODT ($G_{m.p.}/G_0 < 2.8 \times 10^{-4}$),[4] eq 3 yields $\Gamma/\varepsilon_h < 0.01$, which shows that the estimate obtained by setting $\Gamma_a = 0$ in eq 4 is excellent.[18]

Validating a Newns–Anderson-type model for molecular junctions was a topic discussed in some detail in recent works.[18,20,21] To illustrate the fact that this model is also appropriate for the ODT-based junctions fabricated in ref 4, the theoretical I–V curve obtained from eq 1 is presented in Figure 1 along with the raw data for an individual trace measured in ref 4. It is worth emphasizing that, as done in other cases,[20,21] Figure 1 does not simply represent the result of a best fit by constraining the theoretical curve to pass through all the experimental points. The parameters ε_h and Γ[31] needed in eq 1 were been determined by employing only two values deduced from the experimental curve: the transition voltage V_t (the average of the two almost-identical values for positive and negative bias polarities[4]) and the low-bias conductance G. Along with the figures and the discussion presented in the Supporting Information, Figure 1 demonstrates that the Newns–Anderson model excellently describes the I–V measurements on the alkanedithiol-based molecular junctions of ref 4.

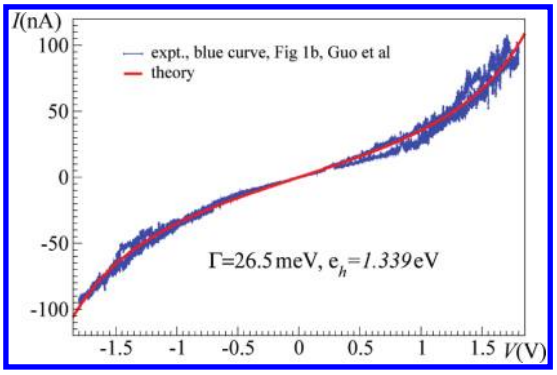

Figure 1. Comparison between an individual experimental curve from ref 4(courtesy of the authors of ref 4) and the theoretical I–V curve obtained via eq 1. Model parameter values determined as described in the main text are given in the inset.

RESULTS AND DISCUSSION

Within the above framework, statistical fluctuations may affect the parameters ε_h and Γ. Therefore, the theoretical analysis should be based on the statistical $p(\varepsilon_h)$ and $q(\Gamma)$ distributions of ε_h and Γ. To couch the discussion in terms as general as possible, no attempt will be made below to identify and characterize in detail sources of microscopic fluctuations for the parameters Γ and ε_h. Inhomogeneous broadening (to be associated here with fluctuations in Γ) is often related to the inability to fabricate perfectly identical single-molecule junctions. Possible sources of fluctuations in ε_h are the softness and distortion of the molecular configuration and the short-range Coulomb interactions at molecule–electrode contacts. The latter aspect has been analyzed in a complementary study.[21]

Experimentally accessible are the conductance and transition voltage histograms $w(g)$ and $v(V_t)$, respectively. These distributions are interrelated. $F(V_t,g)$, the distribution function of V_t and g, can be obtained from eqs 3 and 4 as

$$F(V_t, g) \approx \frac{\sqrt{3}}{4}\varepsilon_h g^{-1/2} p(\varepsilon_h) q(\Gamma) \tag{5}$$

and this yields

$$v(V_t) \equiv \int dg\ F(V_t, g) \approx 0.866 p(\varepsilon_h) \tag{6}$$

$$w(g) \equiv \int dV_t\ F(V_t, g) \approx \frac{1}{2\sqrt{g}}\int d\varepsilon_h\ p(\varepsilon_h) q(\varepsilon_h\sqrt{g})\varepsilon_h \tag{7}$$

Because the experimental V_t distribution is Gaussian,[4] eqs 4 and 6 yield a normal distribution of the HOMO energy offsets whose relative standard deviation $\delta\varepsilon_h$ is equal to that of V_t (i.e., $\delta\varepsilon_h = \delta v_t = \delta V_t/V_t^{m.p.}$):

$$p(\varepsilon_h) = \frac{1}{\varepsilon_h^{m.p.}\delta\varepsilon_h\sqrt{2\pi}}\exp\left[-\frac{(\varepsilon_h/\varepsilon_h^{m.p.} - 1)^2}{2(\delta\varepsilon_h)^2}\right] \tag{8}$$

By fitting the experimental V_t histogram (Figure 5d of ref 4), I obtained a standard deviation $\delta\varepsilon_h = \delta v_t = 23\%$. The dashed (blue) curve depicted in Figure 2 corresponds to the g distribution

$$w(g)|_{\delta\Gamma=0} = \frac{\Gamma_0}{2g}p(\Gamma_0/\sqrt{g}) \tag{9}$$

which was deduced by imposing in eq 7 the condition $q(\Gamma) = \delta(\Gamma - \Gamma_0)$ (i.e., frozen Γ fluctuations; here δ stands for the Dirac "δ function"). The fixed value $\Gamma_0 = \varepsilon_h^{m.p.}(g^{m.p.})^{1/2}$ was adjusted to fit the experimental G maximum. As is visible in Figure 2, fluctuations in ε_h (or, equivalently, V_t) contribute significantly to the width of the G histogram. A standard deviation δv_t amounts to a fwhm of $2.355\delta v_t$ for a normal distribution, and because of the second power of ε_h in eq 3, one

dx.doi.org/10.1021/ja302248h | J. Am. Chem. Soc. XXXX, XXX, XXX–XXX

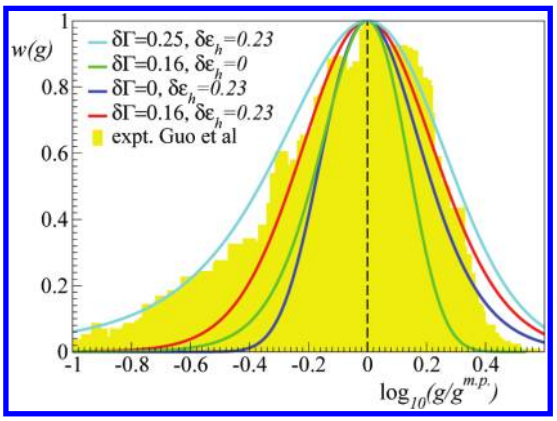

Figure 2. Conductance histograms for ODT-based H-junctions at V = 0.2 V measured experimentally[4] and computed theoretically without ($\delta\Gamma = 0$) and with ($\delta\Gamma$ = 16% and 25%) Γ fluctuations. The significant impact of the ε_h fluctuations on the G histogram should be noted. See the main text for details.

gets for the distribution $w(g)|_{\delta\Gamma=0}$ a fwhm with $\delta g|_{\delta\Gamma=0} = \Delta g/g^{m.p.}|_{\delta\Gamma=0} \sim 4.7\delta\nu_t$. For the above value of $\delta\nu_t$ = 23%, this amounts to $\delta g|_{\delta\Gamma=0} \approx 1.08$, which is not much smaller than the experimental value, $\delta g_{exp} \approx 1.32$.

It is noteworthy that the above conclusion on the important impact of the ε_h fluctuations deduced within the presently adopted framework (the Newns–Anderson model) is different from the statistical interpretation proposed in ref 4.

The statistical analysis of the measured conductance and V_t histograms from ref 4 relies upon three pieces: (i) the assumption that the conductance can be described using Simmons' approach[22] to tunneling, (ii) acceptance of the barrier-shape conjecture ($\varepsilon_h = eV_t$), and (iii) the assumption that the correlations between V_t and G and those between G and the contact conductance A can be quantified by means of the Pearson correlation coefficient. The Pearson coefficient $P(X,Y)$ for two statistical variables X and Y is defined as $P(X,Y) = (\langle XY\rangle - \langle X\rangle\langle Y\rangle)(\langle X^2\rangle - \langle X\rangle^2)^{-1/2}(\langle Y^2\rangle - \langle Y\rangle^2)^{-1/2}$, where $\langle\cdots\rangle$ stands for the statistical average.

Condition (ii) is similar to the present eq 4, but condition (i) substantially differs from eq 3. From (i) and (ii), the dependence $G = A\exp[-(\text{constant})V_t^{1/2}]$ was inferred in ref 4. Because V_t (or ε_h) enters the square root in the above expression, a standard deviation $\delta\nu_t$ yields a relative conductance variance amounting $\delta\nu_t/2$. For a typical value $\delta\nu_t \sim$ 20%, this is ~10%, which is indeed at least 1 order of magnitude smaller than experimentally observed[4] but at the same time much smaller than the value obtained within the Newns–Anderson model. In the latter model, the conductance (eq 3) is expressed in terms of the *square* of ε_h, and therefore, the ε_h fluctuations contribute substantially to the observed G fluctuations, as noted above.

Certainly, Γ fluctuations can also be important. Unfortunately, estimating their impact on the G histograms from the experimental data[4] is not so straightforward as that of the ε_h fluctuations: in general, eq 7 cannot be inverted to deduce $q(\Gamma)$ in terms of the experimentally accessible histograms $p(\varepsilon_h)$ [i. e., $\nu(V_t)$] and $w(g)$. For the benefit of experimentalists, a "modeling flow chart" for a possible approach to data processing is sketched in the Supporting Information. For simplicity, I will also assume here a Gaussian distribution

$$q(\Gamma) = \frac{1}{\Gamma^{m.p.}\delta\Gamma\sqrt{2\pi}}\exp\left[-\frac{(\Gamma/\Gamma^{m.p.}-1)^2}{2(\delta\Gamma)^2}\right] \quad (10)$$

To determine its relative standard deviation $\delta\Gamma$, one can require that the fwhm values of the theoretical $w(g)$ and experimental G histograms coincide (i.e., $\Delta G/G^{m.p.} = 1.32$). The value thus obtained is $\delta\Gamma$ = 16%. The theoretical curve for $w(g)$ obtained by inserting eqs 8 and 10 into eq 7 reasonably reproduces the experimental histogram in the range around the peak, as shown in Figure 2.

As evidence that the effects of ε_h fluctuations on the conductance histograms are altogether ineffective and that fluctuations in the contact conductance are essential, ref 4 invoked the values deduced for the Pearson coefficients, namely, $P_1 \equiv |P(G,V_t)| \ll 1$ and $P_2 \equiv P[\log(G),\log(G/\exp(-V_t^{1/2}))] \approx 1$. However, statistics tells us that the Pearson coefficient $P(X,Y)$ quantifies only the *linear* statistical dependence between X and Y. A large [small] P value $P(X,Y) \approx 1$ [$|P(X,Y)| \ll 1$] can be taken to indicate merely an almost *linear* statistical [in]dependence. For example, with the values $\delta\nu_t = \delta\varepsilon_h$ = 23% and $\delta\Gamma$ = 16%, within the present model [i.e., by using eqs 3, 8, and 10 to compute, e.g., $\langle G\rangle \equiv \int d\varepsilon_h\, d\Gamma\, p(\varepsilon_h)q(\Gamma)G(\varepsilon_h,\Gamma)$] one gets P_1 = 0.10 and P_2 = 0.98, which are consistent with those computed from the experimental data.[4] Nevertheless, as discussed above, the impact of ε_h fluctuations on the G histogram is substantial, and the quantity $G/\exp(-V_t^{1/2})$ has no physical meaning within the Newns–Anderson model.

Although reasonable, the assumption of eq 10 represents only an approximation. It does not allow the shape of the experimental G histograms to be reproduced as accurately as the experimental I–V curves shown in Figure 1 and Figures S1 and S2 in the Supporting Information. Obviously, the actual $q(\Gamma)$ distribution is not Gaussian. With the above choice $\delta\Gamma$ = 16%, the experimental G histogram can be reproduced well in the peak region (say, $|G - G_{m.p.}| \gtrsim G_{m.p.}/2$), but the small-$G$ regime is less satisfactorily described. The small-G region can be better described by larger $\delta\Gamma$ values (which further reduce the Pearson coefficient P_1). Using $\delta\Gamma$ = 25% significantly improves the description at small G values (see Figure 2), but the higher-G regime is less satisfactory reproduced.

The one-dimensional (1D) distribution calculated in Figure 2 does not take full advantage of the two-dimensional (2D) experimental data of ref 4. 2D distributions can also be obtained within the present approach. Figure 3 presents the result of a 2D calculation for $\log_{10}(G/G_0)$ versus V_t. The agreement with the experimental results from Figure 5a of ref 4 is remarkable. The differences between the locations and extensions of the high-probability regions obtained theoretically and experimentally are rather small. The slight experimental asymmetry between positive and negative biases (V_{t+} is slightly different from V_{t-}) can be[20] but has not been included into the theory in order to simplify the analysis. The fact that the theoretical 2D histogram is somewhat more extended than the experimental one at larger G values is related to the fact that the value $\delta\Gamma$ = 25% employed in Figure 2 is good for small G but less appropriate for larger G, as noted above. One should also mention a difference between the theoretical statistical analysis and the experimental one at higher voltages. Theoretically, a statistical event is characterized by a pair (ε_h, Γ) that occurs with a probability $p(\varepsilon_h)q(\Gamma)$, which is assumed to be V-independent. The experimental probability is quantified by the number of "counts" and, as noted in ref 4, the count numbers

dx.doi.org/10.1021/ja302248h | J. Am. Chem. Soc. XXXX, XXX, XXX–XXX

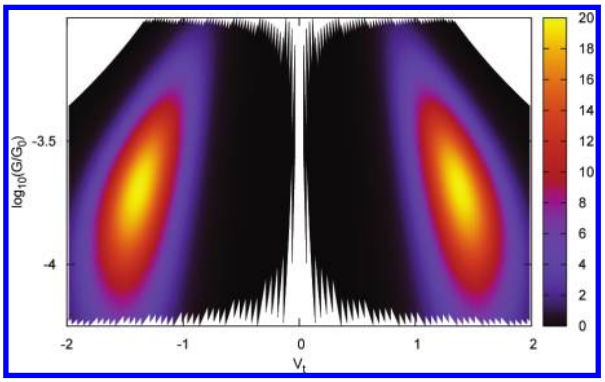

Figure 3. Theoretical 2D distribution $F(V_t g)$ (whose values are given by the various colors) vs $\log_{10}(G/G_0)$ and V_t (in V) calculated within the present approach for $\delta\varepsilon_h = 0.23$, $\delta\Gamma = 0.25$, and the experimental values $G_{m.p.}/G_0 = 2.8 \times 10^{-4}$ and $V_t^{m.p.} = 1.46$ V characterizing the ODT H-junctions of ref 4. It should be noted that the x and y ranges match the upper panel of Figure 5a in ref 4, which is the experimental counterpart of this theoretical histogram.

are smaller at higher V than at lower V. This difference may be reflected in a certain "deformation" of the high-probability regions at higher values of V_t.

An important point to note is that the standard deviations δv_t in refs 4 and 3 were deduced in different ways. The stochastic events of ref 4 are characterized by random g values, and the integrated result $v(V_t)$ is expressed by eq 7. In ref 3, $g = g_{m.p.}$ is fixed, and the V_t histogram is expressed by $F(V_t g_{m.p.})$. Because it represents the product of two distributions [cf. eq 5], its width $\delta\tilde{v}_t$ should be smaller, i.e., $\delta\tilde{v}_t < \delta\varepsilon_h$. The fact that in general the widths in ref 3, $\delta\tilde{v}_t \approx 10\%$ ($<\delta\varepsilon_h$), are smaller than those in ref 4, $\delta v_t = \delta\varepsilon_h \approx 20\%$, can be taken as important support for the present analysis.

SUGGESTIONS FOR ALTERNATIVE DATA PROCESSING

As discussed above, some differences between the theoretical and experimental histograms of Figure 2 indicate departures of the actual Γ distribution from a Gaussian distribution. Unlike the statistical distribution $p(\varepsilon_h)$, which should coincide with the experimental distribution $v(V_t)$ (which is Gaussian,[4] as noted above), $q(\Gamma)$ cannot be directly extracted from experiment. In general, the distribution $q(\Gamma)$ could be a nontrivial function. As shown in eqs 2, $\Gamma = (\Gamma_s\Gamma_t)^{1/2}$ is expressed in terms of two *independent* statistical variables (Γ_s and Γ_t), which characterize the coupling to two independent electrodes.

To extract $q(\Gamma)$ directly, one can suggest a different approach. With the selection of I–V curves having V_t equal to a given value $\overline{V}_t$ (practically, this means having V_t within a range as narrow as possible to permit a reliable statistical analysis) and the construction of G histograms $w(g)|_{\delta\varepsilon_h=0}$ wherein ε_h fluctuations are (practically) suppressed [i.e., $p(\varepsilon_h) \approx \delta(\varepsilon_h - {}^{\sqrt{3}}/_{2}\overline{V}_t)$; green line in Figure 2], then eq 3 gives $\Gamma \approx {}^{\sqrt{3}}/_{2}g^{1/2}\overline{V}_t$, and eqs 2, 4, and 7 yield

$$q(\Gamma) \approx 2\sqrt{g}\,w(g)|_{\delta v_t=0} \tag{11}$$

Information on the Γ (and ε_h) distributions can also be obtained directly, *without* assuming a certain analytical (e.g., Gaussian) expression, using the individual data points g_i and $V_{t,i}$ ($i = 1$–N) from conductance and V_t measurements. Equations 4 and 3 can be utilized to compute relevant averages ($n = 1$) and eventually also higher-order moments ($n \geq 2$), such as $\langle\varepsilon_h{}^n\rangle \approx (1/N)\sum_i V_{t,i}{}^n$, $\langle\Gamma^n\rangle \approx (1/N)\sum_i V_{t,i}{}^n g_i{}^{n/2}$, and $\langle\varepsilon_h{}^n\Gamma^n\rangle \approx (1/N)\sum_i V_{t,i}{}^{2n} g_i{}^{n/2}$ (where the Bessel statistical corrections $N \rightarrow N - 1$ and the factor 1.154 in eq 4 have been omitted for simplicity). In particular, this procedure permits checking of, for example, whether the quantities $\langle\varepsilon_h\Gamma\rangle$ and $\langle\varepsilon_h\rangle\langle\Gamma\rangle$ are equal (i.e., the extent to which the corresponding variables are statistically uncorrelated), as implicitly assumed in the above analysis. A certain correlation between ε_h and Γ cannot be a priori ruled out, and it could contribute to an understanding of, for example, the different HOMO energy offset values deduced from transport and UV photoelectron spectroscopy (UPS) measurements.[10]

CONCLUSION

The present work makes it clear that there is an important difference between the conductance of a molecular junction and its transition voltage. G depends both on the MO energy offset and on the electrode–molecule couplings. The Γ distributions turn out to be not so broad as one could infer by relating them to the strong fluctuations in the contact conductance claimed in ref 4. One can still experimentally distinguish between high-, medium-, and low-conductance junctions (H-, M-, and L-junctions) based on alkanedithiols.[4] There still remain fingerprints of the discontinuous changes in contact geometry, molecular conformation,[4,32−34] or the local electrodes' density of states (cf. eq 2)[35] that would be wiped out by continuous broad Γ distributions. Still, regarding the conductance as a molecular property should be done with care, because it is much more affected by fluctuations in the MO offset than in the transition voltage. The fact that the latter is much less affected (almost an order of magnitude) is important, as it makes V_t a molecular signature, whichs validates TVS as a tool for investigating molecular transport.

In the light of the present study, extending the statistical analysis to other properties appears to be a natural next step. In view of recent advancements in molecular thermoelectricity,[15,36,37] a possible quantity of interest would be the Seebeck coefficient $S = (\pi^2 k_B{}^2 T/3e)\partial \log \mathcal{T}/\partial\varepsilon \approx \pi^2 k_B{}^2 T/(3e\varepsilon_0)$, where T is the temperature and k_B is Boltzmann's constant.[38] Similar to V_t, it should be strongly correlated to ε_0 and should possess a histogram almost identical to that of the latter.

In conclusion, the approach initiated experimentally in ref 4 and developed theoretically in the present paper emphasizes the usefulness of corroborating statistical information on transport properties differently affected by stochastic fluctuations. This should motivate further experimental and theoretical studies, which can significantly contribute to a deeper understanding of the charge transfer in single-molecule devices and characterization of device functions.

ASSOCIATED CONTENT

Supporting Information

Additional figures and details. This material is available free of charge via the Internet at http://pubs.acs.org.

AUTHOR INFORMATION

Corresponding Author

ioan.baldea@pci.uni-heidelberg.de

Notes

The authors declare no competing financial interest.

■ ACKNOWLEDGMENTS

The author thanks Nongjian Tao for his interest in this work, Horst Köppel for valuable discussions, and the Deutsche Forschungsgemeinschaft for financial support.

■ REFERENCES

(1) Song, H.; Reed, M. A.; Lee, T. *Adv. Mater.* **2011**, *23*, 1583−1608.
(2) Wang, G.; Kim, Y.; Na, S.-I.; Kahng, Y. H.; Ku, J.; Park, S.; Jang, Y. H.; Kim, D.-Y.; Lee, T. *J. Phys. Chem. C* **2011**, *115*, 17979−17985.
(3) Lee, W.; Reddy, P. *Nanotechnology* **2011**, *22*, No. 485703.
(4) Guo, S.; Hihath, J.; Diez-Pérez, I.; Tao, N. *J. Am. Chem. Soc.* **2011**, *133*, 19189−19197.
(5) Xu, B.; Tao, N. J. *Science* **2003**, *301*, 1221.
(6) Jang, S.-Y.; Reddy, P.; Majumdar, A.; Segalman, R. A. *Nano Lett.* **2006**, *6*, 2362−2367.
(7) Lörtscher, E.; Weber, H. B.; Riel, H. *Phys. Rev. Lett.* **2007**, *98*, No. 176807.
(8) Scheer, E. In *Handbook of Nanophysics*; Sattler, K., Ed.; CRC Press: Boca Raton, FL, 2010; Vol. *4*, Chapter 37, pp 1−19.
(9) Mishchenko, A.; Vonlanthen, D.; Meded, V.; Bürkle, M.; Li, C.; Pobelov, I. V.; Bagrets, A.; Viljas, J. K.; Pauly, F.; Evers, F.; Mayor, M.; Wandlowski, T. *Nano Lett.* **2010**, *10*, 156−163.
(10) Beebe, J. M.; Kim, B.; Gadzuk, J. W.; Frisbie, C. D.; Kushmerick, J. G. *Phys. Rev. Lett.* **2006**, *97*, No. 026801.
(11) Choi, S. H.; Kim, B.; Frisbie, C. D. *Science* **2008**, *320*, 1482−1486.
(12) Song, H.; Kim, Y.; Jang, Y. H.; Jeong, H.; Reed, M. A.; Lee, T. *Nature* **2009**, *462*, 1039−1043.
(13) Choi, S. H.; Risko, C.; Delgado, M. C. R.; Kim, B.; Brédas, J.-L.; Frisbie, C. D. *J. Am. Chem. Soc.* **2010**, *132*, 4358−4368.
(14) Rampulla, D. M.; Wroge, C. M.; Hanson, E. L.; Kushmerick, J. G. *J. Phys. Chem. C* **2010**, *114*, 20852−20855.
(15) Tan, A.; Sadat, S.; Reddy, P. *Appl. Phys. Lett.* **2010**, *96*, No. 013110.
(16) Huisman, E. H.; Guédon, C. M.; van Wees, B. J.; van der Molen, S. J. *Nano Lett.* **2009**, *9*, 3909−3913.
(17) Araidai, M.; Tsukada, M. *Phys. Rev. B* **2010**, *81*, No. 235114.
(18) Bâldea, I. *Chem. Phys.* **2010**, *377*, 15−20.
(19) Chen, J.; Markussen, T.; Thygesen, K. S. *Phys. Rev. B* **2010**, *82*, No. 121412.
(20) Bâldea, I. *Phys. Rev. B* **2012**, *85*, No. 035442.
(21) Bâldea, I. *Chem. Phys.* **2012**, DOI: 10.1016/j.chemphys.2012.02.011.
(22) Simmons, J. G. *J. Appl. Phys.* **1963**, *34*, 1793−1803.
(23) Bâldea, I. *EPL* **2012**, *98*, No. 17010.
(24) Muscat, J.; Newns, D. *Prog. Surf. Sci.* **1978**, *9*, 1−43.
(25) Schmickler, W. *J. Electroanal. Chem.* **1986**, *204*, 31−43.
(26) Medvedev, I. G. *Russ. J. Electrochem.* **2005**, *41*, 227−240.
(27) Haug, H.; Jauho, A.-P. *Quantum Kinetics in Transport and Optics of Semiconductors*; Springer Series in Solid-State Sciences, Vol. *123*; Springer: Berlin, 1996.
(28) Bâldea, I.; Köppel, H. *Phys. Rev. B* **2010**, *81*, No. 193401.
(29) Li, J.; Tomfohr, J. K.; Sankey, O. F. *Phys. Status Solidi B* **2003**, *239*, 80−87.
(30) Zahid, F.; Paulsson, M.; Datta, S. Electrical Conduction through Molecules. In *Advanced Semiconductors and Organic Nano-Techniques*; Morkoc, H., Ed.; Academic Press: London, 2003; Vol. *3*.
(31) A certain difference between Γ_s and Γ_t can be expected because of the asymmetric scanning tunneling microscope setup, and this leads to a difference between their geometric and arithmetic averages ($\Gamma \leq \Gamma_a$). However, in calculations one can safely use $\Gamma_a = \Gamma$ because the theoretical curves are insensitive to the actual value of Γ_a in the realistic case where $\Gamma_a \ll \varepsilon_h$.
(32) Li, X.; He, J.; Hihath, J.; Xu, B.; Lindsay, S. M.; Tao, N. *J. Am. Chem. Soc.* **2006**, *128*, 2135−2141.
(33) Li, C.; Pobelov, I.; Wandlowski, T.; Bagrets, A.; Arnold, A.; Evers, F. *J. Am. Chem. Soc.* **2008**, *130*, 318−326.
(34) Haiss, W.; Martin, S.; Leary, E.; van Zalinge, H.; Higgins, S. J.; Bouffier, L.; Nichols, R. J. *J. Phys. Chem. C* **2009**, *113*, 5823−5833.
(35) Becker, M.; Berndt, R. *Phys. Rev. B* **2010**, *81*, No. 035426.
(36) Reddy, P.; Jang, S.-Y.; Segalman, R. A.; Majumdar, A. *Science* **2007**, *315*, 1568−1571.
(37) Baheti, K.; Malen, J. A.; Doak, P.; Reddy, P.; Jang, S.-Y.; Tilley, T. D.; Majumdar, A.; Segalman, R. A. *Nano Lett.* **2008**, *8*, 715−719.
(38) Paulsson, M.; Datta, S. *Phys. Rev. B* **2003**, *67*, No. 241403.